Structure and dynamics of the solar wind/ionosphere interface on Mars: MEX-ASPERA-3 and MEX-MARSIS observations

E. Dubinin,[1] R. Modolo,[2] M. Fraenz,[1] J. Woch,[1] F. Duru,[2] F. Akalin,[2] D. Gurnett,[2] R. Lundin,[3] S. Barabash,[3] J. J. Plaut,[4] and G. Picardi[5]

Received 13 March 2008; revised 24 April 2008; accepted 5 May 2008; published 10 June 2008.

[1] The measurements of the local plasma parameters of the ionospheric and solar wind plasmas and the magnetic field strength carried out by the ASPERA-3 and MARSIS experiments onboard Mars Express (MEX) in the subsolar region of the induced Martian magnetosphere provide us with a first test of the pressure balance across the solar wind/ionosphere interface. The structure of this transition is very dynamic and is controlled by the solar wind. For a broad range of the solar wind dynamic pressures, the magnetic field in the boundary layer raises to the values just sufficient to balance the solar wind pressure. The magnetic field frozen into the electrons is transported across the magnetospheric boundary (MB) where solar wind terminates and the planetary plasma begins to prevail. The dense ionospheric plasma has a sharp outer boundary the position of which is usually a little closer to the planet than the MB. Although the number density reaches on this boundary $\sim 10^3$ cm^{-3} the contribution of the ionospheric thermal pressure is rather small and the ionosphere is magnetized. There are also cases when the magnetic field almost does not vary across both boundaries. **Citation:** Dubinin, E., et al. (2008), Structure and dynamics of the solar wind/ionosphere interface on Mars: MEX-ASPERA-3 and MEX-MARSIS observations, *Geophys. Res. Lett.*, *35*, L11103, doi:10.1029/2008GL033730.

1. Introduction

[2] Although it is well established that the direct interaction between solar wind and the Martian exosphere/ionosphere results in the formation of the induced magnetosphere [see, e.g., *Nagy et al.*, 2004; *Dubinin et al.*, 2006] the interface structure near the subsolar point is poorly explored. Information about the characteristics of the Martian ionosphere prior the MEX measurements was rather limited. The only in-situ measurements made by the Viking-1 and 2 landers have shown that the thermal ionospheric pressure is less than the incident solar wind pressure [*Hanson et al.*, 1977] and therefore the picture can be similar to the case of a magnetized ionosphere on Venus. However simultaneous in-situ measurements of the cold and hot plasma components on Mars were absent. The MARSIS sounding experiment on MEX can trace not only ionospheric height profiles below the spacecraft from remote radio sounding, but also can infer the local plasma number density and the magnetic field strength from locally generated plasma echoes [*Gurnett et al.*, 2005, 2007; *Duru et al.*, 2008]. This capability is especially important and significantly increases the resources of MEX (in absence of a magnetometer) for exploring the plasma environment on Mars.

[3] Here we present the first study of the structure of the solar wind/ionosphere interface in the subsolar region of Mars using the simultaneous measurements by the ASPERA-3 and MARSIS experiments onboard the MEX. MEX is in a highly eccentric polar orbit around Mars with periapsis and apoapsis of about 275 and 10000 km, respectively. In-situ plasma and magnetic field measurements by these instruments complement each other and for the first time provide us with the parameters of cold ionospheric and solar wind plasmas, and allow us to determine the pressure components and their balance in this key region.

2. Observations

[4] The ASPERA-3 experiment contains several different instruments for the measurements of plasmas and energetic neutral atoms [*Barabash et al.*, 2006]. The Ion Mass Analyzer (IMA) measures 3D-fluxes of different ion species with m/q resolution (m and q are respectively mass and charge) in the energy range 0.01–36 keV/q. The ELS sensor measures 2D distributions of electron fluxes in the energy range 1 eV–20 keV (the grid usually biased at −5 V protects the sensor from the low energy photoelectrons). Macroscopic parameters of different ion species are determined calculating the moments of ion distribution functions or using a fitting to the Maxwellian distributions [*Fraenz et al.*, 2006]. Since the IMA sensor was not designed for solar wind monitoring the information about the proton component was often limited. Here we used He^{++} ions to monitor the solar wind speed. The solar wind proton number density, which almost equals the total ion density, was evaluated from the electron measurements. The proton bulk speed and temperature could be also determined from ion spectra in many cases.

[5] The MARSIS is the radar sounding ($f \approx 0.1$ to 5.5 MHz) experiment on Mars Express designed to monitor the ionospheric height profile and the subsurface of the planet [*Picardi et al.*, 2004]. However, echoes observed at the electron plasma frequency and its harmonics, and also at the electron cyclotron frequency allow us to measure the local electron density and the magnetic field strength with high accuracy. Although the fundamental plasma frequency ($\omega_{pe} = (4\pi n_e e^2/m_e)^{1/2}$) was not observed directly when the

[1]Max-Planck-Institute for Solar System Research, Katlenburg-Lindau, Germany.
[2]Department of Physics and Astronomy, University of Iowa, Iowa City, Iowa, USA.
[3]Swedish Institute of Space Physics, Kiruna, Sweden.
[4]Jet Propulsion Laboratory, Pasadena, California, USA.
[5]Infocom Department, 'La Sapienza' University of Rome, Rome, Italy.

0094-8276/08/2008GL033730$05.00

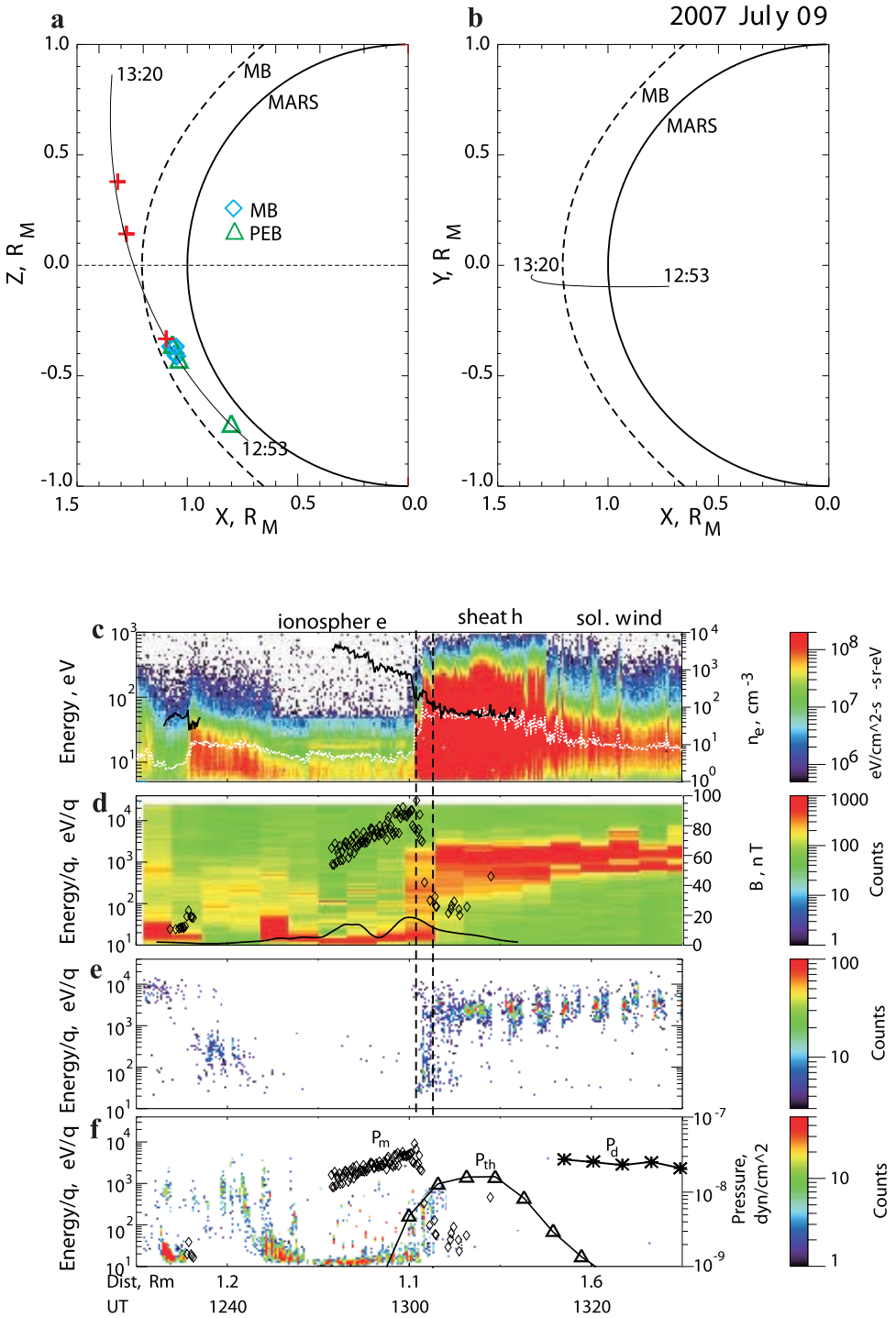

Figure 1. (a) and (b) MEX trajectory in MSO coordinates on July 9, 2007. Trajectories on July 6, 7 and 12 are similar. Symbols show the positions of MB and PEB along these orbits. Red crosses correspond to the distances where pile-up of the magnetic field starts. The dashed curve corresponds to the averaged position of the MB. Energy-time spectrograms of the (c) electrons with the imposed curves of n_e from ASPERA (white) and MARSIS (black) and (d) all ion species, (e) He^{++}, and (f) heavy ($m/q > 16$) ions. Imposed curves are: the magnetic field value from the MARSIS observations (diamonds) and the model (solid) (Figure 1d), the magnetic pressure P_m (diamonds), the thermal proton pressure P_{th} (triangles), and the solar wind ram pressure P_d (asterisks).

electron plasma density was $\leq 1.2 \cdot 10^2$ cm^{-3}, the information about the electron density could be inferred from the spacing of the harmonics. The frequency bandwidth $\Delta f \sim 30$ kHz and the large plasma velocities which can carry the oscillations away from the receiver, impose additional constraints on the density measurements ($n_e \geq 20$–30 cm^{-3}, $V \leq 100$–200 km/s) [*Duru et al.*, 2008]. It is believed [*Gurnett et al.*, 2007] that electron cyclotron echoes at $\Omega_e =$

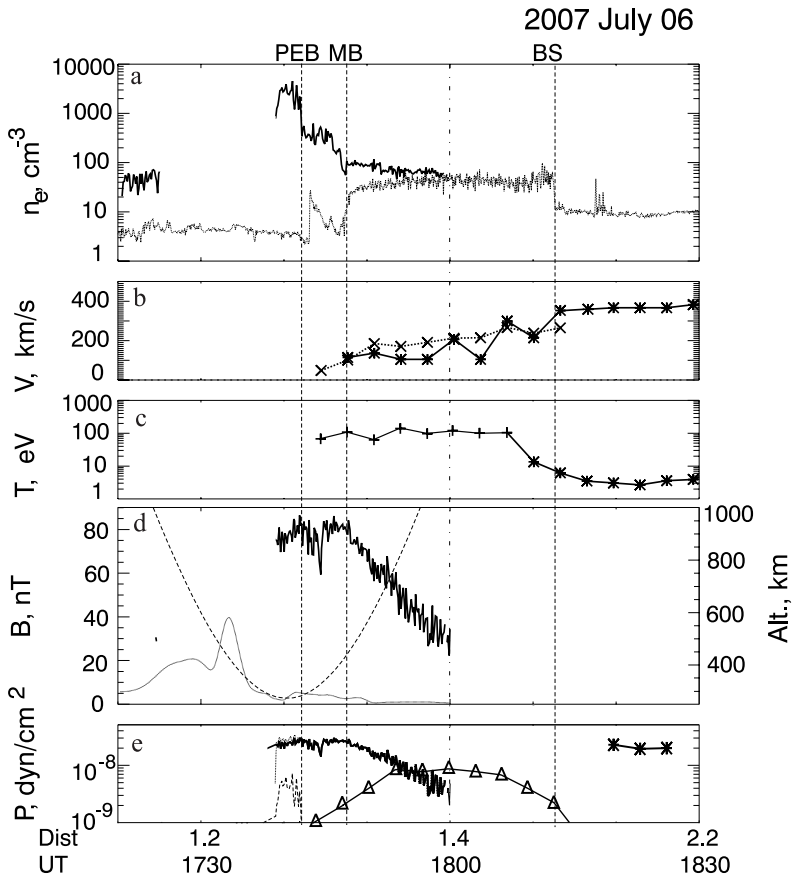

Figure 2. (a) Electron number densities measured by ASPERA-3 and MARSIS, (b) the ion velocities evaluated by different methods, (c) proton temperature, (d) the magnetic field strength (model and observations), and (e) pressures on July 6, 2007.

eB/m_ec which usually are present in the magnetic fields greater than few tens of nT, are excited by the cyclotron motion of the electrons accelerated by the radar wave pulses.

[6] Figures 1a and 1b show the MEX trajectory in MSO coordinates on July 9, 2007. The spacecraft (s/c) moved close to the noon-midnight plane crossing the average position of the magnetospheric boundary (MB) [*Dubinin et al.*, 2006] near the subsolar point. Figure 1 (bottom) presents the energy-time spectrograms of the electrons (Figure 1c) and ions (Figures 1d–1f) measured by the ASPERA-3 sensors. The ion spectrograms correspond to the measurements of all ion species summed over all directions at 192s time resolution (Figure 1d), He^{++} - ions (Figure 1e) and the heavy planetary ions ($m/q > 16$) (Figure 1f) measured at 12 s time resolution. The s/c subsequently crosses the inner magnetosphere void of solar wind ions and electrons, magnetosheath and enters solar wind. The ionosphere is well recognized from the appearance of the energy peaks in the range between 20 and 30 eV on the electron spectrograms due to absorption of the strong HeII line at 30.4 nm in the carbon dioxide dominated atmosphere on Mars [*Frahm et al.*, 2006]. Ions, mainly O^+ and O_2^+, with energies $\leq$20–30 eV also recorded by ASPERA-3 are another signature of the planetary ionosphere. The magnetosheath and solar wind regions are identified from sudden changes in the energy spectra of the electrons and ions. The curves of the electron number density measured by ASPERA-3 and MARSIS, respectively, are superimposed on Figure 1c. MARSIS was able to measure the electron number density not only in the ionosphere but also in a dense magnetosheath plasma providing a reasonable fitting with the ASPERA-3 measurements of a hotter electron component ($E_e > 5$ eV) of solar wind origin. Both curves begin to diverge closer to Mars indicating a dropout of the solar wind and a dominance of a cold ionospheric component inside the magnetosphere. The transition is very sharp ($\sim$25 km, that approximately corresponds to 0.4 c/ω_{pi}, in the normal direction to the static boundary) and accompanied by a sudden jump of the magnetic field value inferred from MARSIS and depicted on Figure 1d (diamonds). This abrupt jump corresponds to the magnetic pile-up boundary (MPB) observed earlier not only on Mars, but also on Venus and comets [*Acuña et al.*, 1998; *Mazelle et al.*, 1989; *Bertucci et al.*, 2003, 2005]. The transition region bounded by the dashed lines is characterized by a mixture of the solar wind and planetary plasmas.

[7] The picture inferred from the orbits on July 6, 7 and 12, 2007 is similar although as it will be shown below, the structure of the interface between the ionosphere and magnetosheath can be different. Figures 2–4 show the structure of this region on three subsequent MEX orbits. They show (a) the electron number density measured by ASPERA-3 (dotted curves) and MARSIS (solid curves),

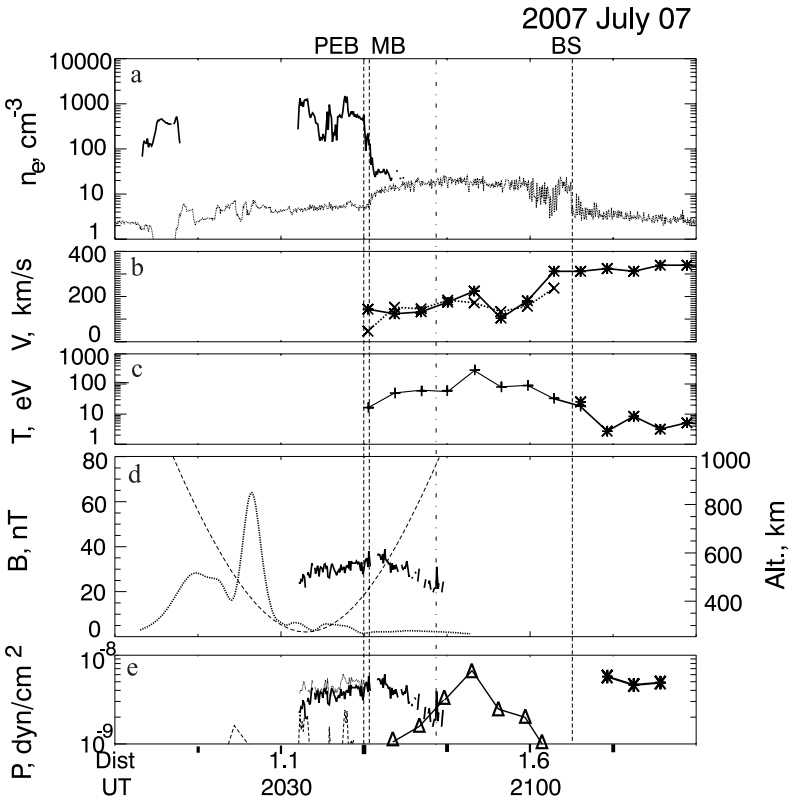

Figure 3. The data on July 7, 2007. The plot setup is as for Figure 2.

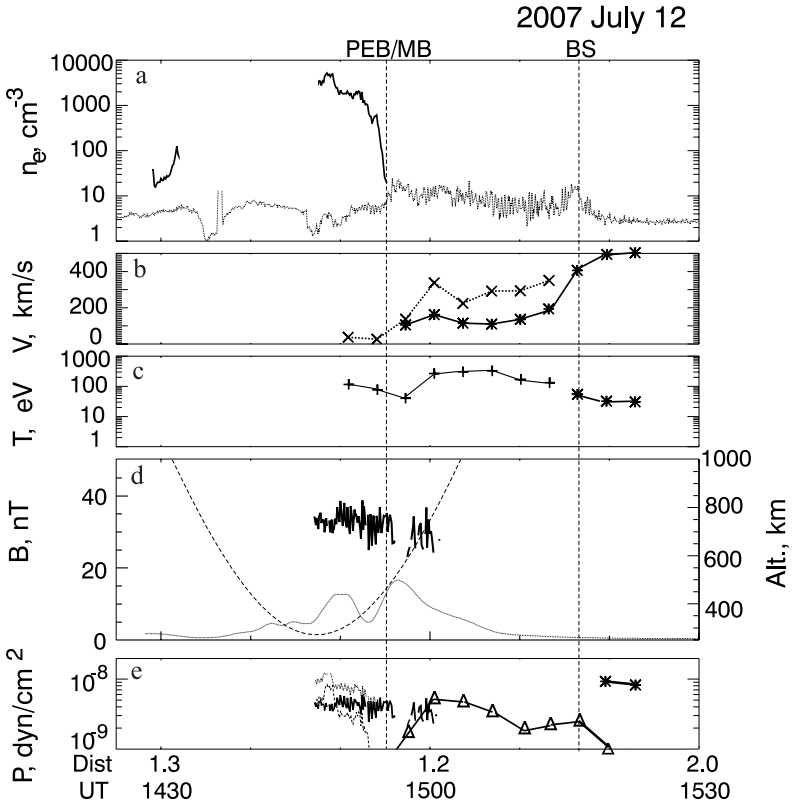

Figure 4. The data on July 12, 2007. The plot setup is as for Figure 2.

(b) the total velocity of He^{++} ions (the star symbols) evaluated from energy-peaks on velocity distribution functions and the proton velocity calculated from the moments of distribution functions (crosses) - this method is more appropriate for the sheath plasma where ion distributions often contain multiple peaks and are not Maxwellian; (c) the proton temperature also evaluated by different methods - in solar wind, a fitting to Maxwellian distributions yields more correct values (star symbols), while in the sheath, the temperature was calculated from integrated moments (crosses); (d) the magnetic field strength inferred from MARSIS (solid curves) and the crustal magnetic field at the MEX position inferred from the Cain model [*Cain et al.*, 2003] to check whether crustal fields are important for the interaction (dotted curves). The s/c altitude is also given (dashed curves). (e) Different pressure components - solar wind dynamic pressure, P_d evaluated as $n_e\, m_p V^2_{He++} \cos^2\phi$ (stars), where n_e, m_p, V_{He++} and ϕ are, respectively, the electron number density, the proton mass, the bulk speed and the solar zenith angle at the position of the magnetospheric boundary; the proton thermal pressure in the sheath (triangles), P_{th} (contribution of the electron pressure in the magnetosheath is significantly less), the magnetic pressure, $P_m = B^2/8\pi$ (thick solid curves), the thermal pressure of a cold ionospheric plasma, $n_{ec}T_c$, where n_{ec} is the electron number density measured by MARSIS. Information about the temperature in the ionosphere $T_c = T_{ec} + T_{ic}$ is very limited. The only reliable measurements of the ion and electron ionospheric temperatures were made on the Viking landers at altitudes <300 km ($T_{ic} \approx T_{ec} \leq 3000$°K) [*Hanson et al.*, 1977, *Hanson and Mantas*, 1988]. Here we use T_c = 1 eV (thin dashed curves). The dotted curves show the sum $B^2/8\pi + n_{ec}T_c$.

[8] Figure 2 depicts the data obtained on the orbit on July 6, 2007. Positions of the bow shock (BS), magnetospheric (MB) and ionospheric boundaries (PEB) are shown by the dashed vertical lines. Note here that MB is defined by the drop in the ELS suprathermal electron density and PEB is the boundary of CO_2 photoelectrons observed on the spectrogram of electron fluxes. In contrast to the previous case, the transition is characterized by a gradual pile-up of the magnetic field which reaches ~80 nT at the MB and then almost does not change. The dashed-dotted line shows tentatively the s/c position at which the pile-up of the magnetic field makes a start. The width of this region along the normal is ~800 km. The total plasma density also gradually increases with a sharp enhancement at the MB. Presently, it is not clear whether the gradual decrease in n_e measured by ASPERA-3 in the broad pile-up region is the effect of mass loading and a change in the ion composition or is caused by the s/c slew at this time. At PEB the electron number density n_e reaches $\sim 3 \cdot 10^3$ cm^{-3}. Such a feature of an abrupt jump in n_e at the PEB is typical for most of the coincident ASPERA-3 and MARSIS observations. We also observe a pressure balance across the MB. The ram solar wind pressure transformed mainly to ion thermal pressure is balanced by the pressure of the pile-up magnetic field. If the temperature of the cold ionospheric component is less than 1 eV then the contribution of the thermal pressure is small in the interface region and the induced magnetic field is the main agent producing an obstacle to solar wind. Note, that a pressure balance is also fulfilled on the orbit on July 9 (Figure 1f).

[9] Figure 3 (orbit on July 7, 2007) presents an example when the solar wind ram pressure was smaller than in the previous cases and pile-up of the magnetic field is weaker (the field strength increases from 22 nT to 35 nT). However the induced field is sufficient to create an obstacle for solar wind. The MB and PEB are close to each other but do not coincide. It is worth noting that the altitude of the MB is ~475 km as compared to 460 km on the orbit on July 6 and 487 km on July 9, i.e. a different structure of the magnetic field pile-up is observed in the same range of altitudes and solar zenith angles.

[10] Figure 4 (July 12, 2007) shows another example where the boundary of a dense and cold ionospheric plasma is sharp and coincides with the boundary of the solar wind stoppage. The remarkable feature is that the magnetic field strength almost does not change across the transition, easily penetrating the ionosphere without a pile-up. The question which forces support the abrupt boundary for solar wind and the ionosphere remains open since the thermal ionospheric pressure is not sufficient unless $T_c \sim 5-10$ eV.

3. Conclusions

[11] The dual-instrument observations performed on the MEX spacecraft in the subsolar region of the solar wind-Mars interaction show that the structure of the solar wind/ionosphere interface can vary a lot. In some cases, the main agent providing the solar wind termination at 450–500 km is the piled-up IMF. The magnetic field raises up to the value sufficient to balance the solar wind pressure. We presented cases when the solar wind ram pressure varies by a factor 5–6 although the position of the magnetospheric boundary almost does not change. The width of this region estimated in the assumption of the stationary picture can also be different varying from 25 to 800 km. There are also cases when the magnetic field almost does not change across the magnetospheric boundary. Such a configuration is probably built in the hemisphere out of which the motional electric field of the solar wind points. Indeed, previous observations and simulations [*Vennerstrom et al.*, 2003; *Modolo et al.*, 2006] show a clear shift of the magnetic barrier to the opposite hemisphere.

[12] Our observations also for the first time show that the transition from the MB to the PEB is accompanied by an increase in the plasma density. A density increase is also observed across the magnetic pile-up boundary. This region contains a mixture of different plasmas and forms the transition from solar wind to the ionospheric plasma. The magnetic field frozen to the electrons is transported through the magnetospheric boundary while the composition and origin of plasma changes drastically.

[13] An important feature is the existence of a rather sharp ionospheric boundary (PEB). Although this boundary was previously tentatively identified from the drop of CO_2 photoelectrons [*Lundin et al.*, 2004; *Dubinin et al.*, 2006] only the MARSIS observations showed that the electron number density abruptly increases on this boundary up to $\sim 10^3$ cm^{-3}. Its existence can be maintained by the inward directed ambipolar electric field driven by a strong increase in the draping of the field lines at and behind the MB

[*Bertucci et al.*, 2003] - central parts of the field lines are anchored in a dense ionosphere while their ends are carried by solar wind.

[14] **Acknowledgments.** Authors (ED, MF) wish to acknowledge support from DFG for supporting this work by grant WO 910/1-1 and DLR by grants 50QM99035, FKZ 50 QM 0801. The research at the University of Iowa was funded by contract 1224107 with the Jet Propulsion Laboratory.

References

Acuña, M. H., et al. (1998), Magnetic field and plasma observations at Mars: Initial results of the Mars Global Surveyor MAG/ER experiment, *Science*, *279*, 1676.

Barabash, S., et al. (2006), The analyzer of space plasma and energetic atoms (ASPERA-3) for the Mars Express mission, *Space Sci. Rev.*, *126*, 113.

Bertucci, C., et al. (2003), Magnetic field draping enhancement at the Martian magnetic pileup boundary from MGS observations, *Geophys. Res. Lett.*, *30*(2), 1099, doi:10.1029/2002GL015713.

Bertucci, C., C. Mazelle, M. H. Acua, C. T. Russell, and J. A. Slavin (2005), Structure of the magnetic pileup boundary at Mars and Venus, *J. Geophys. Res.*, *110*, A01209, doi:10.1029/2004JA010592.

Cain, J., B. Ferguson, and D. Mozzoni (2003), An n = 90 internal potential function of the martian crustal magnetic field, *J. Geophys. Res.*, *108*(E2), 5008, doi:10.1029/2000JE001487.

Dubinin, E., et al. (2006), Plasma morphology at Mars, ASPERA-3 observations, *Space Sci. Rev.*, *126*, 209.

Duru, F., D. Gurnett, D. D. Morgan, R. Modolo, A. F. Nagy, and D. Najib (2008), Electron densities in the upper ionosphere of Mars from the excitation of the electron plasma oscillations, *J. Geophys. Res.*, doi:10.1029/2008JA013073, in press.

Fraenz, M., et al. (2006), Plasma moments in the environment of Mars, Mars Express ASPERA-3 observation, *Space Sci. Rev.*, *126*, 165.

Frahm, R., et al. (2006), Locations of atmospheric photoelectron energy peaks within the Mars environment, *Space Sci. Rev.*, *126*, 389.

Gurnett, D., et al. (2005), Radar soundings of the ionosphere of Mars, *Science*, *310*, 1929, doi:10.1126/science.1121868.

Gurnett, D., et al. (2007), An overview of radar soundings of the Martian ionosphere from the Mars Express spacecraft, *Adv. Space Res.*, *310*, 1929, doi:10.1016/j.asr.2007.01.062.

Hanson, W. C., and G. P. Mantas (1988), Viking electron temperature measurements: Evidence for a magnetic field in the Martian ionosphere, *J. Geophys. Res.*, *93*, 7538.

Hanson, W. C., S. Sanatani, and D. Zuccaro (1977), The Martian ionosphere as observed by the Viking retarding potential analyzers, *J. Geophys. Res.*, *82*, 4351.

Lundin, R., et al. (2004), Solar wind-induced atmospheric erosion at Mars: First results from ASPERA-3 on Mars Express, *Science*, *305*, 1933.

Mazelle, C., et al. (1989), Analysis of suprathermal electron properties at the magnetic pile-up boundary of comet P/Halley, *Geophys. Res. Lett.*, *16*, 1035.

Modolo, R., et al. (2006), Simulated solar wind plasma interaction with the Martian exosphere: Influence of the solar EUV flux on the bow shock and the magnetic pile-up boundary, *Ann. Geophys.*, *24*, 340.

Nagy, A. F., et al. (2004), The plasma environment of Mars, *Space Sci. Rev.*, *11*, 38.

Picardi, G., et al. (2004), Mars Express: A European mission to the red planet, *Eur. Space Agency Spec. Publ., ESA SP-1240*, 51.

Vennerstrom, S., N. Olsen, M. Purucker, M. H. Acuña, and J. C. Cain (2003), The magnetic field in the pile-up region at Mars and its variation with the solar wind, *Geophys. Res. Lett.*, *30*(7), 1369, doi:10.1029/2003GL016883.

F. Akalin, F. Duru, D. A. Gurnett, and R. Modolo, Department of Physics and Astronomy, University of Iowa, Iowa City, IA 52242, USA. (ronan-modolo@uiowa.edu)

S. Barabash and R. Lundin, Swedish Institute of Space Physics, SE-901 87 Kiruna, Sweden. (stas@irf.se; rickard@irf.se)

E. Dubinin, M. Fraenz, and J. Woch, Max-Planck-Institute for Solar System Research, D-37191 Katlenburg-Lindau, Germany. (dubinin@mps.mpg.de)

G. Picardi, Infocom Department, 'La Sapienza' University of Rome, I-00184 Rome, Italy.

J. J. Plaut, Jet Propulsion Laboratory, 4800 Oak Grove Drive, Pasadena, CA 91109, USA.